REPORT DOCUMENTATION PAGE

Form Approved
OMB No. 0704-0188

Public reporting burden for this collection of information is estimated to average 1 hour per response, including the time for reviewing instructions, searching existing data sources, gathering and maintaining the data needed, and completing and reviewing this collection of information. Send comments regarding this burden estimate or any other aspect of this collection of information, including suggestions for reducing this burden to Department of Defense, Washington Headquarters Services, Directorate for Information Operations and Reports (0704-0188), 1215 Jefferson Davis Highway, Suite 1204, Arlington, VA 22202-4302. Respondents should be aware that notwithstanding any other provision of law, no person shall be subject to any penalty for failing to comply with a collection of information if it does not display a currently valid OMB control number. **PLEASE DO NOT RETURN YOUR FORM TO THE ABOVE ADDRESS.**

1. REPORT DATE *(DD-MM-YYYY)*	**2. REPORT TYPE**	**3. DATES COVERED** *(From - To)*
	Final Performance Report	5/15/2008 – 5/14/2012

4. TITLE AND SUBTITLE

Optical Transformers with Integrated Couplers (OTIC) for Ultrahigh SERS Enhancement

5a. CONTRACT NUMBER

5b. GRANT NUMBER
FA9550-08-01-0257

5c. PROGRAM ELEMENT NUMBER

6. AUTHOR(S)
Professor Ming C. Wu

5d. PROJECT NUMBER

5e. TASK NUMBER

5f. WORK UNIT NUMBER

7. PERFORMING ORGANIZATION NAME(S) AND ADDRESS(ES) AND ADDRESS(ES)
University of California,
Berkeley
2150 Shattuck Ave RM313
Berkeley, CA 94704-5940

8. PERFORMING ORGANIZATION REPORT NUMBER

9. SPONSORING / MONITORING AGENCY NAME(S) AND ADDRESS(ES)
AF Office of Scientific Research
875 N. Randolph Street RM3112
Arlington VA 22203

10. SPONSOR/MONITOR'S ACRONYM(S)
AFOSR

11. SPONSOR/MONITOR'S REPORT NUMBER(S)
AFRL-OSR-VA-TR-2012-1131

12. DISTRIBUTION / AVAILABILITY STATEMENT

DISTRIBUION A: APPROVED FOR PUBLIC RELEASE

13. SUPPLEMENTARY NOTES

14. ABSTRACT

We have developed a fundamental understanding of the electromagnetic enhancement in surface-enhanced Raman spectroscopy (SERS) that enable us to design and fabricate nano-antenna arrays on silicon wafers using nanofabrication technologies compatible with current silicon CMOS foundries. We have developed three generations of optical antennas with increasing enhancement factors. The final nano-arch antennas exhibit a strong enhancement of 1.7x10^10. These antennas can potentially be fabricated on 12-inch wafers using standard optical lithography in CMOS foundries.

15. SUBJECT TERMS

16. SECURITY CLASSIFICATION OF:			**17. LIMITATION OF ABSTRACT**	**18. NUMBER OF PAGES**	**19a. NAME OF RESPONSIBLE PERSON**
a. REPORT	**b. ABSTRACT**	**c. THIS PAGE**			**19b. TELEPHONE NUMBER** *(include area code)*

Standard Form 298 (Rev. 8-98)
Prescribed by ANSI Std. Z39.18

DARPA SERS F&T Final Report
January 13, 2012

Optical Antenna Engineering For SERS

PI : Prof. Ming Wu
University of California, Berkeley

The long-range goal of this project is to develop ultra-sensitive SERS (Surface-Enhanced Raman Spectroscopy) probes with reproducible enhancement factors. To achieve this goal, we suggest impedance matched optical antennas with ultra-small mode volume (uniform sub-10 nm gap) on metal ground plane for maximum field enhancement.

For theoretical understanding, the field enhancement of an optical antenna at resonance has been derived using coupled mode theory (CMT) as:

$$\frac{|E_{loc}|^2}{|E_i|^2} = \frac{2A_c\lambda_{res}}{\pi}\frac{Q}{Q_{rad}}\frac{Q}{V_{eff}} \quad (1)$$

where E_{loc} and E_i are the local field amplitude at the high field region of an optical antenna and the field amplitude of incoming excitation beam, respectively, V_{eff} is the effective mode volume of the resonator, and A_c is the maximum effective aperture of the antenna which is determined by spatial mode matching between the antenna radiation pattern and the excitation beam pattern. The antenna's total quality factor (Q) is the summation of radiation quality factor (Q_{rad}) and absorption quality factor (Q_{abs}): $Q^{-1} = Q_{rad}{}^{-1} + Q_{abs}{}^{-1}$. This equation gives an intuitive picture that the field enhancement of an optical antenna is proportional to two important factors: antenna efficiency (Q/Q_{rad}) and Purcell enhancement factor[19] (Q/V_{eff}). Using the equation for the field enhancement, there are two main parameters that can be optimized to achieve maximum field enhancement: 1) The maximum field enhancement condition is achieved when Q_{rad} becomes equal to Q_{abs} ($Q_{rad} = Q_{abs}$). 2) The effective mode volume of the antenna (V_{eff}) needs to be reduced, which can be achieved by shrinking the size of antenna feed gap.

At the end of Phase II, we had demonstrated dipole antenna array controlling radiation resistance by the thickness of dielectric spacer layer between antenna and ground plane, enabling impedance matching for maximum power transfer. The measured maximum SERS enhancement using *trans*-1,2-two (4-pyridyl) ethylene (BPE) as the target molecule at optimum impedance matching condition was 1.14×10^9. However, the dipole antenna fabricated using conventional e-beam lithography has a technical limit, which makes it difficult to reduce the antenna gap below 10 nm. In Phase 3, we focused on the development of manufacturable optical antennas with higher enhancement factors. We have investigated two antenna structures whose gaps (< 5 nm) can be precisely defined by a thin dielectric layer rather than by electron-beam lithography, which has poor uniformity and reproducibility. The first structure is optical patch antenna (Fig. 1). It

consists of a nanopatch on top of a ground plane. High field is concentrated in the 2nm gap between the patch and the ground plane. The gap spacing is precisely controlled by atomic layer deposition (ALD). The measured SERS intensity is 6x better than our Phase 2 antenna (EF ~ $7x10^9$). The patch antenna, however, has poor radiation efficiency as we reduce the gap to nanometer scale as the image currents in ground plane cancel the antenna current.

To overcome the trade-off between radiation efficiency and small gap spacing, we have developed a new "arch-dipole antenna". The two arms of a dipole antenna are shorted by a tall, narrow arch (Fig. 2a). It has been verified by FDTD simulation that the arch-dipole antenna has two main modes depending on the current distribution and both modes show good ability of light energy confinement at the antenna gap (Fig. 2b). Since, the current distribution in the arch structure plays an important for the arch antenna mode, the antenna can be optimized by adjusting the arch height (Fig. 3). Our simulations show that a field enhancement of 4.6×10^{10} is achievable with gold arch-dipole antenna with 1 nm gap, and 3.4×10^{11} with silver antenna (Fig. 4). The antenna gap (inside the arch) can now be defined by the thickness of a sacrificial dielectric layer using spacer lithography (Fig. 5a). The dielectric layer thickness is again controlled by ALD to sub-nm accuracy. The SEM image in Fig. 5b shows the fabricated optical antennas aligned on 5 nm wide fins. Fig. 6a shows that the reflection spectra of the antenna arrays. The resonance dip exhibits a red shift with increasing antenna length, as expected. Fig. 6b shows the SERS spectra from antenna arrays with various lengths. The strongest Raman signals are observed from 210 nm and 240 nm long antenna arrays, which have resonances near the excitation and Stokes shifted wavelength, respectively. The measured enhancement factor from the strongest SERS signal is $1.7x10^{10}$. The strong dependence on the excitation polarization confirms that the SERS signals are from the optical antennas (Fig. 6c). Since the proposed new antennas can be made by deep UV lithography, uniform SERS substrates with sub-5nm gaps can be mass produced in existing Si CMOS foundries (Fig. 7).

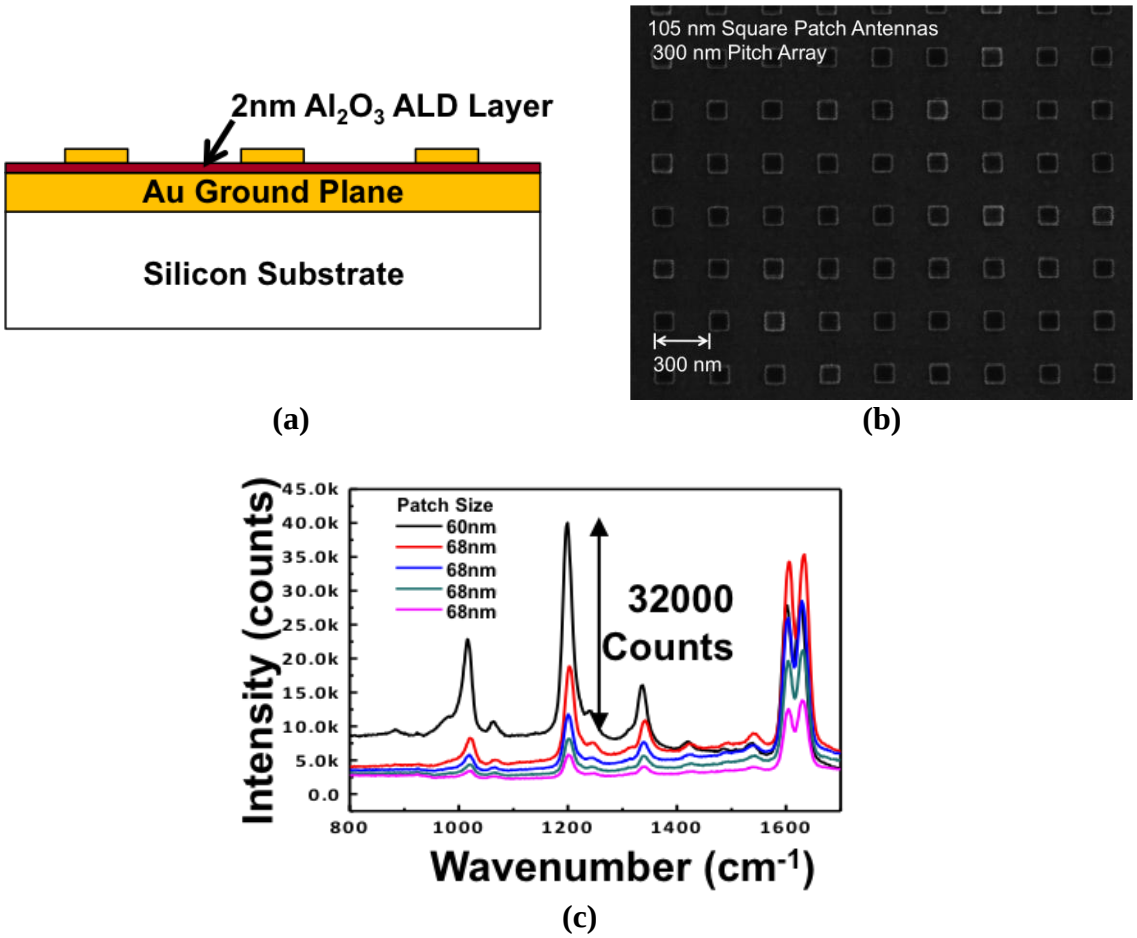

Figure 1. (a) The schematic picture of patch antenna array. (b) SEM image of fabricated patch antenna. (c) BPE SERS measurement (10 sec integration).

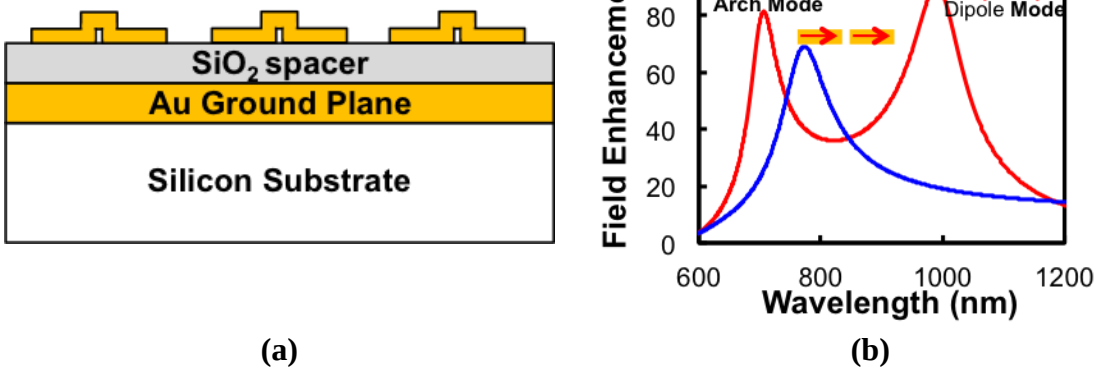

Figure 2. (a) The schematic picture of arch-dipole antenna array. (b) Field enhancement simulation comparison of arch-dipole antenna and dipole antenna. Red and blue lines show the field enhancement of arch-dipole antenna and dipole antenna, respectively. The arch-dipole antenna clearly shows two main modes depending on the current direction at the arch structure.

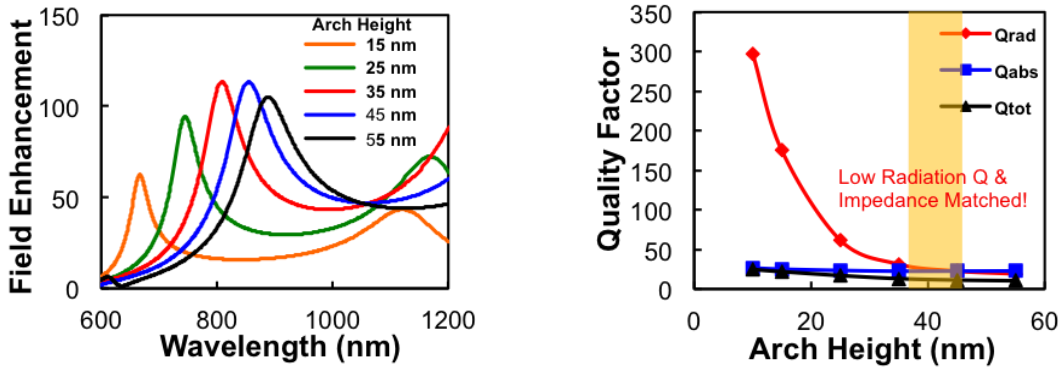

(a) **(b)**

Figure 3. (a) Field enhancement simulation of arch-dipole antennas with various arch heights. (b) Quality factor plot as a function of arch height. Low radiation Q and impedance matching condition can be achieved with 5 nm gap spacing.

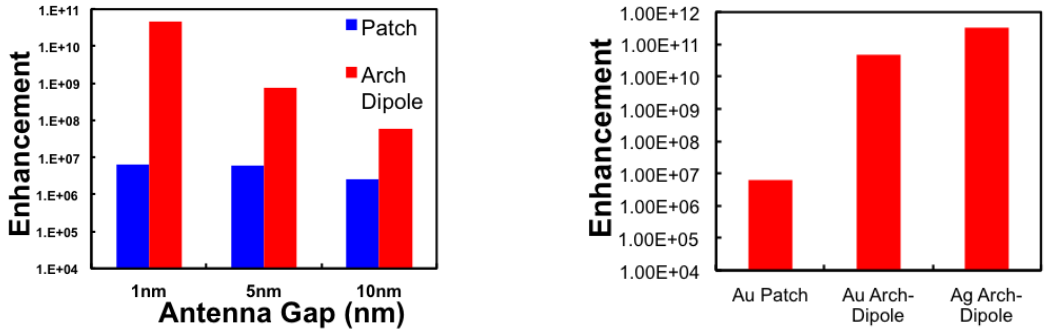

(a) **(b)**

Figure 4. (a) Field enhancement comparison between patch antenna and arch-dipole antenna. Field enhancement of arch-dipole keeps increasing with antenna gap scaling down. (b) Field enhancement comparison of 1 nm gap gold patch antenna, gold arch-dipole antenna and silver arch-dipole antennas. (FDTD simulations)

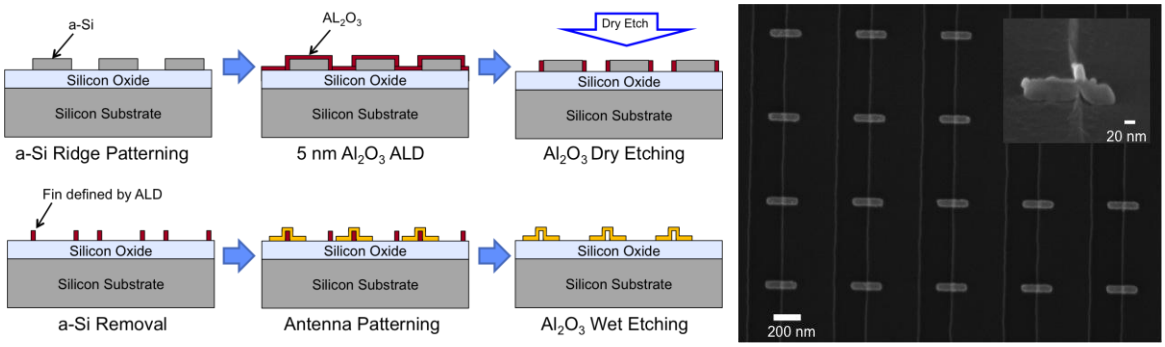

(a) **(b)**

Figure 5. (a) Fabrication process of arch-dipole antenna array. (b) SEM images of optical antenna array aligned on 5 nm fins. Inset shows perspective view of a single antenna.

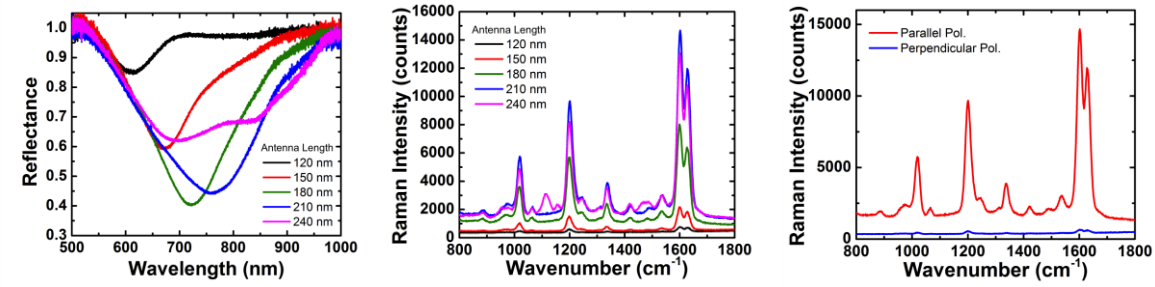

(a) **(b)** **(c)**

Figure 6. (a) Reflectance measurement of fabricated optical antenna arrays with antenna length variations. (b) Measured BPE SERS spectra. (c) SERS comparison with two different excitation polarizations.

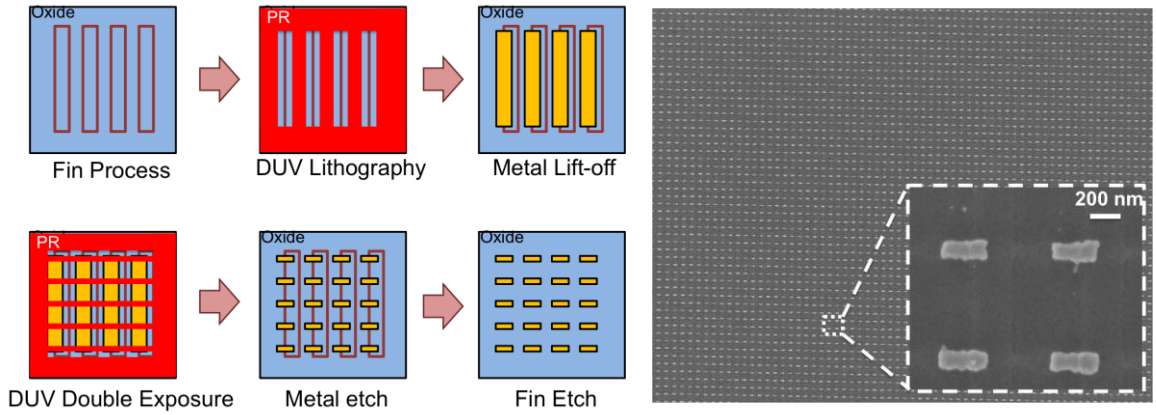

(a) **(b)**

Figure 7. (a) Developed wafer-scale fabrication process using deep-UV (DUV) photo lithography. (b) SEM picture of the large area optical antenna array fabricated on 6 inch wafer.